JACS
JOURNAL OF THE AMERICAN CHEMICAL SOCIETY
Communication
pubs.acs.org/JACS

Colloidal Synthesis of Wurtzite Cu_2ZnSnS_4 Nanorods and Their Perpendicular Assembly

Ajay Singh,[†,‡] Hugh Geaney,[†] Fathima Laffir,[†] and Kevin M. Ryan*[,†,‡]

[†]Materials and Surface Science Institute (MSSI), Department of Chemical and Environmental Sciences, University of Limerick, Limerick, Ireland

[‡]SFI Strategic Research Cluster in Solar Energy Research, University of Limerick, Limerick, Ireland

Supporting Information

ABSTRACT: The quaternary copper chalcogenide Cu_2ZnSnS_4 is an important emerging material for the development of low-cost and sustainable solar cells. Here we report a facile solution synthesis of stoichiometric Cu_2ZnSnS_4 in size-controlled nanorod form (11 nm × 35 nm). The monodisperse nanorods have a band gap of 1.43 eV and can be assembled into perpendicularly aligned arrays by controlled evaporation from solution.

Colloidal semiconductor nanocrystals are a remarkable material set that can be synthesized and processed as a "chemical" in high yield while exhibiting optical and electronic properties that are size-dependent.[1] Applications ranging from biolabeling to photocatalysis and photovoltaics that exploit either the discrete or collective properties of these size-controlled crystals have emerged.[2] The synthesis of the archetypal binary (II−VI) nanocrystals has progressed to the point where precise control over their size, shape, composition, and crystal phase has become routine, thereby rapidly accelerating the advances that utilize these as building blocks.[1b,3] Extension of colloidal nanocrystal synthesis to ternary and quaternary semiconductors has the capacity to expand this research platform greatly.[4,5]

In particular, copper-based ternary and quaternary semiconductors such as $CuInS_2$ (CIS), $CuIn_xGa_{1-x}Se_2$ (CIGS), and Cu_2ZnSnS_4 (CZTS) are of interest because of their high absorption coefficients, low toxicities, and band gaps suitable for solar energy conversion.[4−6] Advances in the colloidal synthesis and shape control of CIS and CIGS nanocrystals have been demonstrated, although similar reports for CZTS remain elusive.[4c−e] CZTS has been flagged as the material most likely to allow unrestricted photovoltaic application on a global scale, given the relatively abundant nature of Zn and Sn in comparison with In and Ga and the promising efficiencies of 9.7%.[6,7] Generating CZTS in nanocrystal form allows absorber layer production by simple solution processes (spin-casting, spraying, or printing methods), dramatically offsetting the cost of expensive vacuum processes.[6b,7,8] While synthesis of zero-dimensional (0D) CZTS nanocrystals in the tetragonal crystal structure has been achieved,[5a−e] their formation in the more attractive rod geometry remains elusive. In nanorods, maximization of total absorption and directional charge transfer is possible by controlling the length while retaining the diameter-dependent properties such as band gap. Moreover, control of orientation and positioning such that each nanorod is vertically aligned and close-packed allows their collective properties to be harnessed at the device scale.[9−11]

Herein we describe a colloidal synthesis of monodisperse stoichiometric CZTS nanorods in high yield. The quaternary semiconductor nanorods have the wurtzite crystal structure with elongation occurring along the [002] direction and exhibit a band gap of 1.43 eV. This crystal phase is not just attractive for shape control but is also known to allow wide-range tuning of the band gap as a result of the random distribution of In/Sn and Ga/Zn ions in the crystal structure.[4f,g,5f] We further demonstrate the subsequent assembly of the rods into superstructures with each rod close-packed and oriented orthogonal to the substrate. The rod geometry, hierarchical assembly, and optimal crystal structure make this route of significant interest for low-cost photovoltaic devices.

In a typical synthesis, copper(II) acetylacetonate (0.261 g, 1 mmol), zinc acetate (0.091 g, 0.5 mmol), tin(IV) acetate (0.177 g, 0.5 mmol), and trioctylphosphine oxide (1.353 g, 3.5 mmol) were mixed with 10 mL of 1-octadecene in a three-neck round-bottom flask and evacuated at room temperature for 30−45 min. The solution was then heated to 240−260 °C under an argon atmosphere. At 150−160 °C, a mixture of 0.25 mL of 1-dodecanethiol (1-DDT) and 1.75 mL of *tert*-dodecyl mercaptan (t-DDT) was quickly injected into the flask, resulting in an immediate color change from dark-green to wine-red and then finally to brown. After injection, the reaction was allowed to proceed for 15−30 min with continuous stirring. Nanorod growth was terminated by removal of the heating mantle, and at 80 °C, 2−4 mL of anhydrous toluene was added to the mixture to quench the reaction. The nanorods were then washed in 1:1 toluene/ethanol and centrifuged at 4000 rpm for 10 min to yield a brownish centrifuged product.

The dark-field scanning transmission electron microscopy (DF-STEM) image in Figure 1a shows that the nanorods were formed with good monodispersity, having an average length of 35 ± 3 nm and diameter of 11 ± 0.5 nm. The as-synthesized CZTS nanorods were predominantly bullet-shaped with ∼7% polydispersity, which could be improved by size-selective precipitation. The polycrystalline selected-area electron diffraction (SAED) pattern (Figure 1a inset) is indexed with rings to (002), (101), and (102), corresponding to the wurtzite phase of CZTS. High-resolution TEM (HRTEM) images of an

Received: November 30, 2011
Published: January 30, 2012

   dx.doi.org/10.1021/ja2112146 | J. Am. Chem. Soc. 2012, 134, 2910−2913

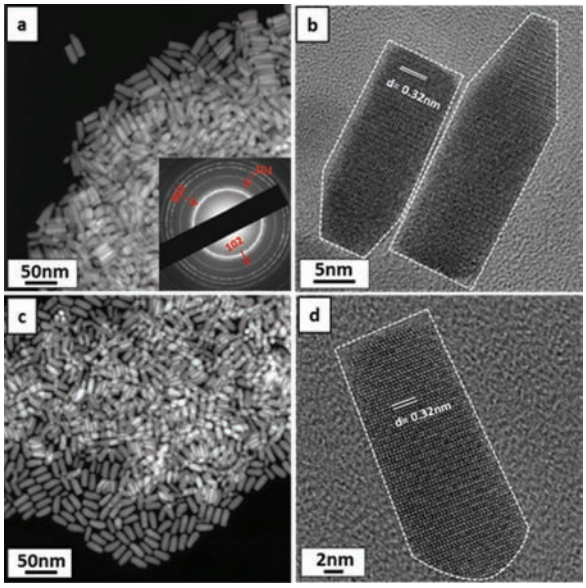

Figure 1. (a) DF-STEM image of bullet-shaped CZTS nanorods. The inset shows the corresponding SAED pattern. (b) HRTEM image showing that the bullet-shaped CZTS nanorods are elongated in the [002] direction. (c) DF-STEM image of CZTS nanorods synthesized in the presence of a higher 1-DDT concentration. (d) HRTEM image of a single CZTS nanorod from (c).

individual bullet-shaped nanorod (Figure 1b) showed lattice fringes with a spacing of d = 0.32 nm, which corresponds to the (002) lattice plane of the wurtzite CZTS structure. This growth direction along the c axis is characteristic of the wurtzite phase,[3a,c,4c−e] and its preferred formation in this synthesis, rather than kesterite, is critical to elongation. The key for stabilizing the wurtzite phase rather than kesterite is the use of dodecanethiol in the reaction, as it acts as both a sulfur source and a ligand. Dodecanethiol has been previously reported as a strong coordinating ligand for the wurtzite copper-based chalcogenide nanocrystals CIS and CIGS.[4c−g,5f] While studying the effect of thiols (1-DDT and t-DDT) on the formation of wurtzite CZTS nanocrystals, we observed that a combination of the two is necessary for the nanorods to form. In addition, single-phase CZTS nanorods were formed only when the thiols were injected at a temperature of <200 °C to avoid the formation of unwanted Cu_2S side products. Syntheses carried out in the presence of only 1-DDT [for details, see the Supporting Information (SI)] yielded only smaller pseudospherical wurtzite CZTS nanocrystals (Figure S1 in the SI). Conversely, when the concentration of 1-DDT in the reaction mixture was doubled, the shape of the CZTS nanocrystals changed from bullet-shaped to more conventional rod-shaped (Figure 1c). This suggests that 1-DDT binds more strongly to facets other than (002), allowing anisotropic growth in this direction. The HRTEM image of an individual rod-shaped CZTS nanorod (Figure 1d) shows clear lattice fringes with d = 0.32 nm, corresponding to the (002) lattice planes of the wurtzite structure.

X-ray diffraction (XRD) was employed as a bulk analysis technique to ensure compositional homogeneity across the nanorod samples. A resultant XRD diffractogram (Figure 2a) shows major reflections at 2θ values corresponding to the (100), (002), (101), (102), (110), (103), and (112) planes of a hexagonal structure and matching well with those of the previously reported CZTS wurtzite structure.[5f] This structure

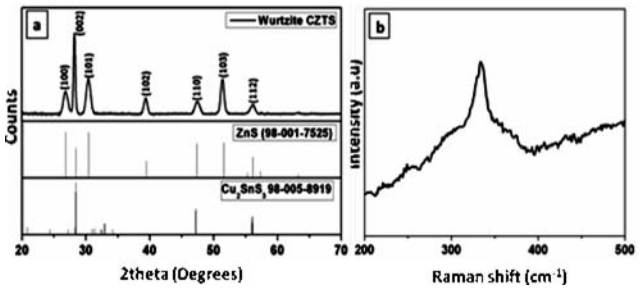

Figure 2. (a) XRD pattern of as-synthesized wurtzite CZTS nanorods. For reference, the XRD patterns of wurtzite ZnS (PCPDF no. 98-001-7525) and monoclinic Cu_2SnS_3 (PCPDF no. 98-005-8919) are also shown. (b) Raman spectrum of CZTS nanorods.

can be derived from wurtzite ZnS by substitution of Zn with Cu and Sn atoms.[5f] In particular, the XRD pattern of wurtzite CZTS matches the combined reflections from hexagonal ZnS and monoclinic Cu_2SnS_3, as shown in Figure 2a. The single Raman peak at 333 cm^{-1} is close to the value reported for bulk CZTS (Figure 2b).[12] The noted broadening of the Raman peak has been seen previously for nanocrystals and is due to the phonon confinement within the nanocrystal.[13] It is noticeable that there are no additional peaks for other phases such as ZnS, SnS, and Cu_2S, which confirms the single phase of the CZTS nanorods.

X-ray photoelectron spectroscopy (XPS) was performed to investigate the chemistry of the CZTS nanorods. A survey spectrum of the synthesized nanorods identified the presence of Cu, Zn, Sn, S, O and C (Figure S2). High-resolution spectra of Zn 2p, Cu 2p, Sn 3d, and S 2p were measured to determine the oxidation states of the constituent elements (Figure 3). The

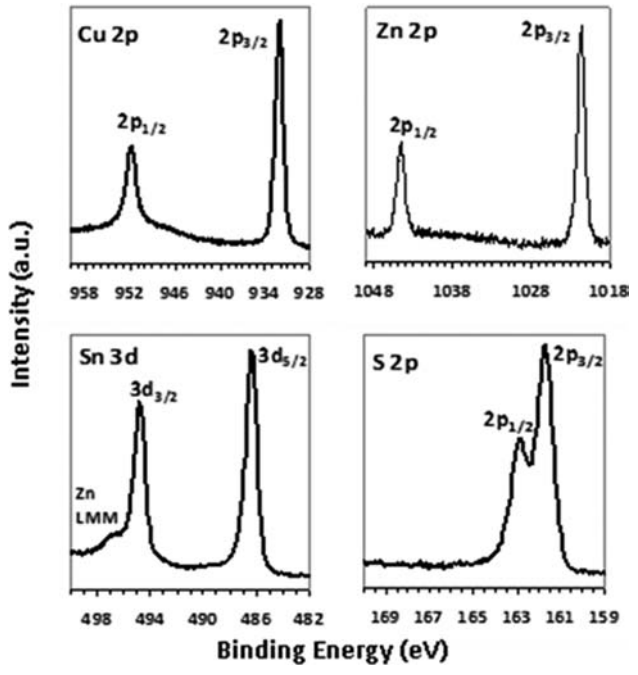

Figure 3. High-resolution XPS analysis of CZTS nanorods.

narrow doublet peaks in the Cu 2p spectrum appear at 932.1 eV ($2p_{3/2}$) and 951.9 eV ($2p_{1/2}$); the peak separation of 19.8 eV is indicative of Cu(I).[14,4b] The peaks of Zn 2p appear at binding energies of 1021.6 and 1044.7 eV, which can be assigned to

dx.doi.org/10.1021/ja2112146 | J. Am. Chem. Soc. 2012, 134, 2910−2913

Zn(II) with a peak splitting of 23.1 eV.[4a] The Sn(IV) state was confirmed by peaks located at 486.4 and 494.8 eV with its characteristic peak separation of 8.4 eV.[14,15] The sulfur spectrum can be assigned to the presence of sulfides at binding energies of 161.7 and 162.9 eV with a doublet separation of 1.2 eV.[14,15] Also, to investigate the quantitative analysis of all four elements in the nanorods, a scanning electron microscope equipped with an energy-dispersive X-ray spectroscopy (EDS) detector was used to find the Cu:Zn:Sn:S stoichiometric ratio, which was close to 2:1:1:4 (Figure S3), corresponding well with the elemental ratio of CZTS.

The as-synthesized CZTS nanorods have high uniformity across the length and diameter, which is a prerequisite for self-assembly. We have recently shown with wurtzite (II–VI) nanorods that the simplest method to achieve perpendicular assembly is to create conditions under which the rods preorganize in solution. At an optimal concentration, the inter-nanorod distance in solution is sufficient to allow attractive interparticle interactions such as dipole–dipole to overcome the Coulombic repulsion, resulting in nucleation and growth of 2D-assembled sheets.[10c,d] The CZTS rods have a ζ potential of 5 ± 2 mV and a permanent dipole along the [002] direction. Therefore, simply modulating the nanorod concentration over a range allows the isolation of the critical concentration for preferential assembly (Figure S4). The top-down DF-STEM image in Figure 4a shows a 3D superstructure

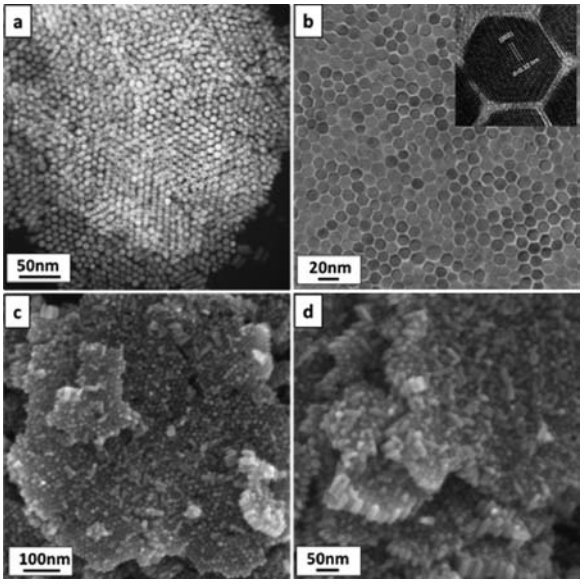

Figure 4. (a) DF-STEM image showing a 3D superstructure of CZTS nanorods. (b) Top-down HRTEM image showing the closed-packed monolayer of CZTS nanorods. The inset shows an HRTEM image of a single nanorod. (c, d) Scanning electron microscopy (SEM) and HRSEM images showing top-down and side views of a multilayer assembly of CZTS nanorods.

of CZTS nanorods. Figure 4b shows a TEM image of a monolayer of vertically oriented CZTS nanorods in which the perfect close-packed hexagonal ordering can be seen. The inset top-down HRTEM image of a single nanorod shows the spacing of the lattice fringes to be d = 0.32 nm, which matches the (002) plane of the wurtzite structure of CZTS nanorods. When the rate of evaporation of the solvent is controlled, the 2D sheets can be deposited sequentially to form 3D multilayer arrays, as shown in Figure 4c,d. Assemblies up to micrometer-sized areas can also be obtained by this approach (Figure S5). The direct optical band gap of CZTS nanorods was calculated from the UV–vis spectrum (Figure 5) to be 1.43 eV by

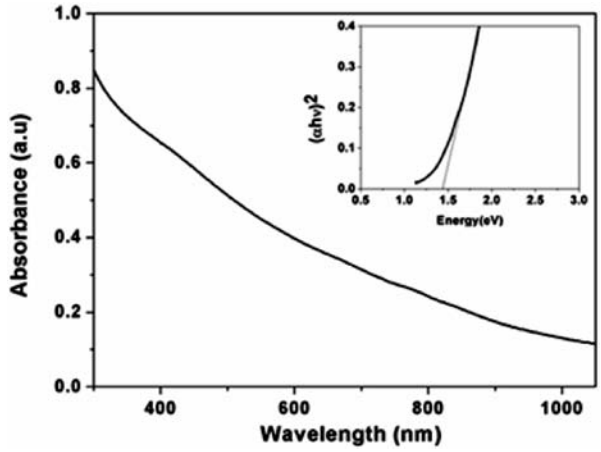

Figure 5. UV–vis absorption spectrum of the CZTS nanorods and (inset) determination of the band gap.

extrapolation of the linear region of a plot of $(\alpha h\nu)^2$ versus energy, where α represents the absorption coefficient and $h\nu$ is the photon energy.[5f]

In conclusion, a reproducible method for solution synthesis of high-quality monodisperse wurtzite Cu_2ZnSnS_4 nanorods has been reported. The rods are defect-free single crystals with a band gap in the visible part of the electromagnetic spectrum. The constituent elements of these rods are nontoxic and highly abundant, allowing for a wide range of low-cost applications exploiting their absorption or emission properties (e.g., biolabels, fluorescent emitters, or photocatalysis). Their facile organization into close-packed and vertically oriented arrays on the substrate strengthens their potential for use as solar absorber layers, where directional orientation and length control will likely allow for enhanced efficiencies.[9b,c,16]

■ ASSOCIATED CONTENT

Supporting Information

Experimental details; TEM images and XRD pattern of pseudospherical wurtzite CZTS nanocrystal, EDX and XPS survey spectra, concentration study for perpendicular assembly of CZTS nanorods, and additional SEM images of assembly. This material is available free of charge via the Internet at http://pubs.acs.org.

■ AUTHOR INFORMATION

Corresponding Author

Kevin.m.ryan@ul.ie

Notes

The authors declare no competing financial interest.

■ ACKNOWLEDGMENTS

This work was supported by Science Foundation Ireland (SFI) through the Principal Investigator Program (Contract 06/IN.1/I85) and the Solar Energy Conversion Strategic Research Cluster (07/SRC/B1160). This work was also conducted under the framework of the INSPIRE Project, funded by the Irish Government's Program for Research in Third Level Institutions, Cycle 4, National Development Plan 2007-2013.

REFERENCES

(1) (a) Alivisatos, A. P. *Science* **1996**, *271*, 933. (b) Talapin, D. V.; Lee, J. S.; Kovalenko, M. V.; Shevchenko, E. V. *Chem. Rev.* **2010**, *110*, 389.

(2) (a) Bruchez, M.; Moronne, M.; Gin, P.; Weiss, S.; Alivisatos, A. P. *Science* **1998**, *281*, 2013. (b) Sanyal, A.; Bala, T.; Ahmed, S.; Singh, A.; Piterina, A. V.; McGloughlin, T. M.; Laffir, F. R.; Ryan, K. M. *J. Mater. Chem.* **2009**, *19*, 8974. (c) Chen, X.; Shen, S.; Guo, L.; Mao, S. S. *Chem. Rev.* **2010**, *110*, 650. (d) Gur, I.; Fromer, N. A.; Geier, M. L.; Alivisatos, A. P. *Science* **2005**, *310*, 46.

(3) (a) Peng, X. G.; Manna, L.; Yang, W. D.; Wickham, J.; Scher, E.; Kadavanich, A.; Alivisatos, A. P. *Nature* **2000**, *404*, 59. (b) Regulacio, M.; Han, M. *Acc. Chem. Res.* **2010**, *43*, 621. (c) Yin, Y.; Alivisatos, A. P. *Nature* **2005**, *437*, 664.

(4) (a) Guo, Q.; Kim, S. J.; Kar, M.; Shafarman, W. N.; Birkmire, R. W.; Stach, E. A.; Agrawal, R.; Hillhouse, H. W. *Nano Lett.* **2008**, *8*, 2982. (b) Norako, M. E.; Franzman, M. A.; Brutchey, R. L. *Chem. Mater.* **2009**, *21*, 4299. (c) Kruszynska, M.; Borchert, H.; Parisi, J.; Kolny-Olesiak, J. *J. Am. Chem. Soc.* **2010**, *132*, 15976. (d) Wang, Y.-H. A.; Zhang, X.; Bao, N.; Lin, B.; Gupta, A. *J. Am. Chem. Soc.* **2011**, *133*, 11072. (e) Lu, X.; Zhuang, Z.; Peng, Q.; Li, Y. *CrystEngComm* **2011**, *13*, 4039. (f) Qi, Y.; Liu, Q.; Tang, K.; Liang, Z.; Ren, Z.; Liu, X. *J. Phys. Chem. C* **2009**, *113*, 3939. (g) Pan, D.; An, L.; Sun, Z.; Hou, W.; Yang, Y.; Yang, Z.; Lu, Y. *J. Am. Chem. Soc.* **2008**, *130*, 5620. (h) Connor, S. T.; Hsu, C.-M.; Weil, B. D.; Aloni, S.; Cui, Y. *J. Am. Chem. Soc.* **2009**, *131*, 4962. (i) Koo, B.; Patel, R. N.; Korgel, B. A. *J. Am. Chem. Soc.* **2009**, *131*, 3134. (j) Norako, M. E.; Brutchey, R. L. *Chem. Mater.* **2010**, *22*, 1613. (k) Steinhagen, C.; Akhavan, V. A.; Goodfellow, B. W.; Panthani, M. G.; Harris, J. T.; Holmberg, V. C.; Korgel, B. A. *ACS Appl. Mater. Interfaces* **2011**, *3*, 1781.

(5) (a) Riha, S. C.; Parkinson, B. A.; Prieto, A. L. *J. Am. Chem. Soc.* **2009**, *131*, 12054. (b) Zou, C.; Zhang, L. J.; Lin, D. S.; Yang, Y.; Li, Q.; Xu, X. J.; Chen, X. A.; Huang, S. M. *CrystEngComm* **2011**, *13*, 3310. (c) Guo, Q.; Ford, G. M.; Yang, W.-C.; Walker, B. C.; Stach, E. A.; Hillhouse, H. W.; Agrawal, R. *J. Am. Chem. Soc.* **2010**, *132*, 17384. (d) Riha, S. C.; Parkinson, B. A.; Prieto, A. L. *J. Am. Chem. Soc.* **2011**, *133*, 15272. (e) Larsen, T. H.; Sigman, M.; Ghezelbash, A.; Doty, R. C.; Korgel, B. A. *J. Am. Chem. Soc.* **2003**, *125*, 5638. (f) Lu, X.; Zhuang, Z.; Peng, Q.; Li, Y. *Chem. Commun.* **2011**, *47*, 3141. (g) Shavel, A.; Arbiol, J.; Cabot, A. *J. Am. Chem. Soc.* **2010**, *132*, 4514. (h) Norako, M. E.; Greaney, M. J.; Brutchey, R. L. *J. Am. Chem. Soc.* **2012**, *134*, 23. (i) Deka, S.; Genovese, A.; Zhang, Y.; Miszta, K.; Bertoni, G.; Krahne, R.; Giannini, C.; Manna, L. *J. Am. Chem. Soc.* **2010**, *132*, 8912. (j) Zhuang, Z. B.; Peng, Q.; Zhang, B.; Li, Y. D. *J. Am. Chem. Soc.* **2008**, *130*, 10482.

(6) (a) Wadia, C.; Alivisatos, A. P.; Kammen, D. M. *Environ. Sci. Technol.* **2009**, *43*, 2072. (b) Habas, S. E.; Platt, H. A. S; van Hest, M. F. A. M.; Ginley, D. S. *Chem. Rev.* **2010**, *110*, 6571. (c) van Hest, M. F. A. M. Ginley, D. S. Future Directions for Solution-Based Processing of Inorganic Materials. In *Solution Processing of Inorganic Materials*; Mitzi, D. B., Ed.; Wiley: Hoboken, NJ, 2008.

(7) Todorov, T. K.; Reuter, K. B.; Mitzi, D. B. *Adv. Mater.* **2010**, *22*, E156.

(8) (a) Sargent, E. H. *Nat. Photonics* **2009**, *3*, 325. (b) Guo, Q.; Hillhouse, H. W.; Agrawal, R. *J. Am. Chem. Soc.* **2009**, *131*, 11672.

(9) (a) Hu, J. T.; Li, L. S.; Yang, W. D.; Manna, L.; Wang, L. W.; Alivisatos, A. P. *Science* **2001**, *292*, 2060. (b) Krahne, R.; Morello, G.; Figuerola, A.; George, C.; Manna, L. *Phys. Rep.* **2011**, *501*, 75. (c) Gonzalez-Valls, I.; Lira-Cantu, M. *Energy Environ. Sci.* **2009**, *2*, 19.

(10) (a) Ahmed, S.; Ryan, K. M. *Chem. Commun.* **2009**, 6421. (b) Ryan, K. M.; Mastroianni, A.; Stancil, K. A.; Liu, H. T.; Alivisatos, A. P. *Nano Lett.* **2006**, *6*, 1479. (c) Singh, A.; Gunning, R. D.; Sanyal, A.; Ryan, K. M. *Chem. Commun.* **2010**, *46*, 7193. (d) Singh, A.; Gunning, R. D.; Ahmed, S.; Barrett, C. A.; English, N. J.; Garate, J.-A.; Ryan, K. *J. Mater. Chem.* **2012**, *22*, 1562. (e) Zanella, M.; Gomes, R.; Povia, M.; Giannini, C.; Zhang, Y.; Riskin, A.; van Bael, M.; Hens, Z.; Manna, L. *Adv. Mater.* **2011**, *23*, 2205.

(11) (a) Baker, J. L.; Widmer-Cooper, A.; Toney, M. F.; Geissler, P. L.; Alivisatos, A. P. *Nano Lett.* **2010**, *10*, 195. (b) Ahmed, S.; Ryan, K. M. *Nano Lett.* **2007**, *7*, 2480. (c) Baranov, D.; Fiore, A.; vn Huis, M.; Giannini, C.; Falqui, A.; Lafont, U.; Zandbergen, H.; Zanella, M.; Cingolani, R.; Manna, L. *Nano Lett.* **2010**, *10*, 743. (d) Kelly, D.; Singh, A.; Barrett, C. A.; O'Sullivan, C.; Coughlan, C.; Laffir, F. R.; O'Dwyer, C.; Ryan, K. M. *Nanoscale* **2011**, *3*, 4580.

(12) Fernandes, P. A.; Salome, P. M. P.; da Cunha, A. F. *Thin Solid Films* **2009**, *517*, 2519.

(13) Bersani, D.; Lottici, P. P.; Ding, X. *Appl. Phys. Lett.* **1998**, *72*, 73.

(14) NIST-XPS database, version 3.5. http://srdata.nist.gov/xps/ (accessed Nov 30, 2011).

(15) Moulder, J. F.; Stickle, W. F.; Sobol, P. E.; Bomben, K. D. *Handbook of X-Ray Photoelectron Spectroscopy*; Perkin-Elmer: Eden Prairie, MN, 1992.

(16) (a) Kriegel, I.; Rodriguez-Fernandez, J.; Como, E. D.; Lutich, A. A.; Szeifert, J. M.; Feldmann, J. *Chem. Mater.* **2011**, *23*, 1830. (b) Wang, J.-J.; Xue, D.-J.; Guo, Y.-G.; Hu, J.-S.; Wan, L.-J. *J. Am. Chem. Soc.* **2011**, *133*, 18558. (c) Kriegel, I.; Jiang, C.; Rodríguez-Fernández, J.; Schaller, R. D.; Talapin, D. V.; da Como, E.; Feldmann, J. *J. Am. Chem. Soc.* **2012**, *134*, 1583.